Mathematical Models of the Proteasome Product Size Distribution

Fabio Luciani[1] and Alexey Zaikin[2]

[1] School of Biotechnology and Biomolecular Sciences, University of New South Wales, 2026 Sydney, Australia
[2] University of Potsdam, Am Neuen Palais 10, 14469 Potsdam, Germany

Zusammenfassung The proteasome is a barrel-shaped multi-subunit protease involved in the degradation of the Ubiquitin-tagged proteins. Here we review two models which investigate an influence of a length dependent cleavage and transport processes on the outcome of a digestion experiment. The first model describes the kinetics of the proteasome degradation, the second is focused on the translocation properties of the protein inside the proteasome. Both these approaches, mesoscopic and microscopic ones, lead to the explanation of the experimentally observed nonmonotonous proteasome product size distribution.

Self-organization is an immanent property of all complex biological systems [5]. Two basic principles can lie behind the mechanisms of the self-organization. First, self-organization can appear due to the effects of nonlinear dynamics [5], where one have the interaction between elements with dynamics described by nonlinear functions. Second, self-organization can occur due to the intrinsic stochasticity of biological systems following the new ideas of statistical physics [7,6]. In the latter case, the properties of noise can be exploited even to increase the level of the order in the dynamical system. Following these two principles in the present paper we discuss two mathematical models which describe the proteasome function.

Proteasomes are multicatalytic cellular protease complexes that degrade intracellular proteins into smaller peptides. Many roles in the cell's metabolism are played by proteasomes: they destroy abnormal and misfolded proteins tagged with Ubiquitin and are an essential component of the ATP-Ubiquitin-dependent pathway for protein degradation [3]. Proteasomes play an important role in the immune system by generating antigenic peptides of 8-12 residues to be presented by the MHC class I molecules and, hence, are the main supplier of peptides for its recognition by killer T-cells [13,15,23,9]. Proteasome inhibition has been suggested as a promising new target for cancer treatment [19].

One of the important experimental result that describes the proteasome function is a length distribution of the fragments obtained in vitro experiments. For long substrates it was found that this dependence typically is nonmonotonous and has a single peak around the length of 7-12 amino acids (aa) for practically all types of the proteasome [18,17,12,2]. This length of peptides is the most requested length for a normal functioning of the immune system. The mechanism behind such a length distribution is not completely clear. It was widely believed that the proteasome degrades proteins according to the "molecular ruler"

to yield products of rather uniform size. It was proposed [26] that peptides of 7–9 residues were generated as a result of coordinated cleavages by neighboring active sites. However, evidence for the molecular ruler is quite limited because the maximum in the length distribution is smoothed and not pronounced as a sharp peak [12]. It is also interesting to note that in some experiments three peak length distributions have been found [14]. Several theoretical models for the kinetics of proteasome degradation have been published. Some of the models describe the degradation of short peptides with qualitatively different kinetics [24,25,22] or small number of cleavage positions [11]. The theoretical model [11,20] for the degradation of long substrates is applied to specific proteins with predefined cleavage sites and is fitted to experimental data describing the fragment quantity after proteasomal degradation.

Here we review two models which describe the influence of a length dependent cleavage, in- and efflux rates, and transport processes on the outcome of a digestion experiment. The first model describes the proteasome kinetics [16], the influx of the substrate, the cleavage process, and the efflux of the fragments. It captures also the opening and closing of the proteasome gate and explains a three-peak length distribution of products as observed experimentally [14]. The second model [27,28] addresses solely the protein translocation and shows that the differences in the length dependent velocity rates can be important and that the nonmonotonous translocation rate function can result in one or three peak length distributions.

1 Kinetic model of the the proteasome

The model. The model describes the rates at which the concentrations of fragments of length k change over time. The concentrations change by proteasomal cleavage, making two short fragments out of a long one, and by the influx and efflux of fragments through the gates. The dynamics does not depend on the amino acid sequence and orientation of the fragment, but only depends on the length of the fragment. Let n_k and N_k be the concentration of fragments of length k inside and outside the proteolytic chambers. Then,

$$\frac{dN_k}{dt} = -a(k)\Big[1 - v\sum_{j=1}^{L} jn_j\Big]N_k + e(k)n_k \ , \tag{1}$$

$$\begin{aligned}\frac{dn_k}{dt} &= a(k)\Big[1 - v\sum_{j=1}^{L} jn_j\Big]N_k - e(k)n_k \\ &\quad -c\sum_{i=1}^{k-1} F_{k,i}n_k + c\sum_{j=k+1}^{L}(F_{j,k} + F_{j,j-k})n_j \ ,\end{aligned} \tag{2}$$

for $k = 1, 2, \ldots, L$. The substrate N_L is an outside fragment of length $k = L$. The first term of 1 describes the influx of fragments into the proteasome. For the influx function $a(k)$ we consider the case where there is no re-entry of fragments

Parameter	Description	Dimension	Default value
L	Length of the Substrate	amino acids	100
$N_L(0)$	Initial substrate concentration	mol	100
$\hat{a}$	Rate of influx	time^{-1}	0.1
$\hat{e}$	Rate of efflux	time^{-1}	1
c	Cleavage rate	time^{-1}	1
θ	Critical fragment length	amino acids	25
μ	Preferred cleavage position	amino acids	9
σ	Std of cleavage position	amino acids	3
v	Scaling factor	-	1/200

Tabelle1. Parameters values of the kinetic model.

other than the substrate, i.e., we set $a(k) = \hat{a}$ for $k = L$, and $a(k) = 0$ otherwise. The influx of substrate into the proteolytic chambers is a rate limiting factor in protein degradation. Experimental works have suggested that the influx is limited by the maximum amount of amino acids that can be accommodated in the proteasome (see [16] and refs therein). In our model the influx rate therefore decreases when the total amount of amino acids inside, $\sum_{k=1}^{L} kn_k$, increases. The maximum filling of the proteasome is normalized to one by a scaling parameter v determining the maximum number of amino acids that can be accommodated within the CP.

We assume that the influx does not strongly depend on the amino acid composition of the substrate. Based on the intuition that each peptide binds with a probability p to the gate subunits, hence impairing the passage through the narrow pore, it has been proposed that the efflux rate is a negative exponent of the length $exp(-\gamma n)$ where $\gamma = \frac{1}{1-p}$ and n is the fragment's length [11]. On the other hand, the analysis of *in vitro* digestion of 25 and 27 aa long substrates performed with the 20S proteasome suggests a length dependent reprocessing rate which decreases with the increase of the substrate length. These data suggest an increasing Hill function with high exponent to describe the reduced cleavage rate for short substrates [21]. Hence, we describe the efflux rate with a phenomenological Hill function with high exponent and a critical length $\theta = 25$ aa $e(k) = \hat{e}/(1 + (k/\theta)^{10})$. The efflux rate switches at a fragment length of $k \simeq \theta$ from the maximal efflux rate $\hat{e} = 1$ for short fragments to an efflux close to zero for long fragments (see 1A).

The first two terms of 2 are the same influx and efflux terms as discussed above. The last terms describe the cleavage machinery located in the core of the proteasome. Fragments of length k are cut at a maximum rate c and with probability $0 < F_{k,i} < 1$ into two fragments of length i and $k - i$. Two terms account for the loss and for the gain of each fragment of length k. The negative term corresponds to a loss for fragments of length k which are cut in shorter fragments, and the positive term is a gain because fragments of length $j > k$ can be cleaved into a fragment of length k. For parameters see Table 1.

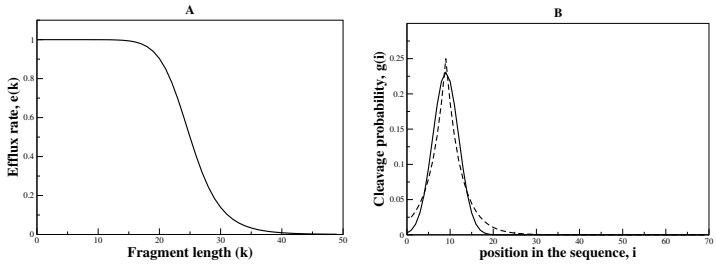

Abbildung1. A. The efflux rate. **B.** Binomial (dashed lines) and gaussian (solid lines) distributions for the cleavage probability.

The main assumption for the cleavage mechanism is that the proteasome cleaves proteins starting around their N-termini or C-termini. It has been suggested that there is a preferred length of 7-9 aa for an optimal docking of the substrate with the binding grooves during the cleavage process inside the CP [10]. We therefore assume that the proteasome starts at a distance $m \simeq 9$ from one end of the protein/peptide, and scans the substrate chain in both directions until a cleavage site is found. One can model [16] the cleavage probability with a phenomenological binomial or a Gaussian distribution, as here.

The model has three rate parameters: the cleavage rate c, the maximum influx rate $\hat{a}$, and the maximum efflux rate $\hat{e}$. A normal time scale of proteasome experiments is minutes. However, experimental results on proteasome degradation are typically compared for a certain level of substrate degradation, rather than at a specific point in time. Since time is not an important issue, one can always rescale the time such that $c = 1$ per time unit. Increasing the cleavage rate will therefore be the same as decreasing the flux through the gates (i.e., as decreasing $\hat{a}$ and $\hat{e}$). For details of the simulation algorithm see [16].

Kinetics. Experimental data suggest that the *in vitro* degradation rate of substrates by the proteasome obeys Michaelis-Menten kinetics (see [16] and refs therein). For long substrates the maximum degradation rate and the Michaelis-Menten constant are known to decrease with the length of the substrate. Our model also exhibits Michaelis-Menten kinetics (see 2). For various initial substrate concentrations, 2 depicts the depletion of the substrate ($L = 100$) in the solution (Panel A), and the corresponding filling of the proteasome (Panel B). There is a rapid initial phase during which the proteasome fills up by influx of the substrate. At the very early stage of degradation, due to the filling of the proteasome, the substrate loss is not linear. When the initial substrate concentration is low this initial phase accounts for a significant depletion of the substrate concentration N_L (see 2A). Otherwise, the substrate concentration remains high and the filling of the proteasome approaches a quasi steady state corresponding to a maximum degradation rate.

To study the Michaelis-Menten kinetics, we fix the substrate concentration by fixing $N(t) = N(0)$ and let the model approach the corresponding steady

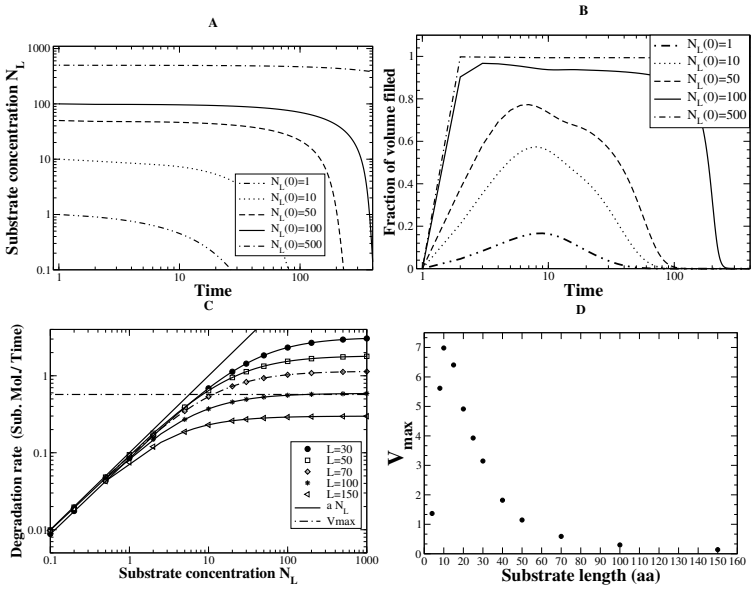

Abbildung2. A. Substrate consumption for a different initial concentration, $N_L(0)$. **B.** Filling of the proteasome core particle (in amino acids). **C.** Michaelis-Menten log-log plot; each symbol-curve denotes a substrate of a different length obtained from the model presented in Eqs. (1, 2) in conditions where the proteasome is in a bath of substrate in order to prevent substrate limiting effects. The solid line is given by the initial slope $\hat{a}N_L$ and the dashed-dot line is the V_{max}, both predicted with the simplified model (see [16]) for the standard parameter values (see Table 1) and an average efflux $\bar{e} = 0.2$. **D.** V_{max} as a function of the substrate length. It increases for substrate shorter than 10 aa and decreases for longer substrates. The initial substrate concentration is $N_L(0) = 6000$.

state. At the steady state we measure the degradation rate as the number of substrate molecules in solution which are lost per unit time, and depict that as a function of the substrate concentration and the length of the substrate, L (see 2C). This reveals a family of Michaelis-Menten curves for the various lengths of the substrate. The longer the substrate, the smaller the maximum degradation rate, V_{max}, and the smaller the Michaelis-Menten constant, K_m. The degradation rate at low substrate concentrations is fairly independent on the length of the substrate (see 2C).

Fig. 2D shows the maximum degradation rate V_{max}, calculated numerically from the full model Eqs. (1, 2), as a non-linear function of the substrate length. It increases for small substrates with a maximum at ca. 10 aa and decreases with the inverse of the length for longer substrates. Very small fragments are weakly degraded because of the low cleavage rate for fragments shorter than 9 aa. This explains why the degradation rate decreases for very short fragments. For longer fragments, V_{max} was found to decrease with the inverse of the length.

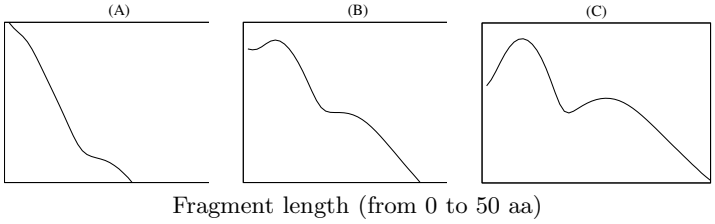

Abbildung3. Length distributions of the fragments outside the proteasome. From left to right the efflux rate $\hat{e}$ increases $\hat{e} = (0.1, 1, 10)$. Each distribution has been taken at the time 170 (A), 86 (B), 76 (C) when 20 % of substrate degraded. The vertical on each plot is the log frequency (from 0 to 0.25). The influx rate $\hat{a} = 0.01$. Note that the distributions are insensitive to the variation in the influx rate $\hat{a}$ [16].

This is due to the fact that the CP volume is finite and thus the influx decreases with the increase of the substrate length. Therefore, the degradation rate decreses accordingly. This compares well with experimental results (see [16] and refs therein). Interestingly, the ratio of V_{max}/K_m increases with the increase of the substrate length [4] and saturates for long substrates reaching 50% of its maximum for substrate of 23 aa which indicating that both constants decrease with the length of the substrate in the same ratio.

Length distribution of the fragments. *In vitro* experiments generate cleavage products that range from 2 to 35 aa with an average length of $7-8$ aa (see [16] and refs therein). Using size exclusion chromatography and on-line fluorescence detection, [14] showed that the products generated by the wild type (WT) proteasome have a length distribution with three broad peaks corresponding to lengths of $2-3$, $8-10$, and $20-30$ aa, respectively.

In 3 we show how the fragment length distribution depends on the size of the gate, i.e., on the influx and efflux rates $\hat{a}$ and $\hat{e}$, as calculated with the model Eqs. (1, 2). For an intermediate efflux rate, we obtain three-peaked distributions similar to those observed in experiments [14] for a wide range of influx rates. Note that the first peak has its maximum at 1 aa but we call this decreasing slope "peak" for simplicity. In our model, the three-peaked distributions are the result of the cleavage machinery, which tends to cut fragments of $8-10$ aa, and the efflux of products, which favors the short fragments.

In the Panel A the efflux is slow compared to the cleavage ($c/\hat{e} = 10$). As a consequence, most substrate molecules are fragmented extensively before they are exported, and one observes short fragments in the solution. Increasing the efflux rate 10-fold (the panel B) gives a similar time scale to the efflux and to the cleavage, and allows for a three-peak distribution. Another 10-fold increase of the efflux rate (see Panel C) makes cleavage the limiting factor. The ratio of long to short fragments increases. Because the residence time of fragments in the CP is short, there is less fragmentation, and the first peak at 1-3 aa decreases.

Abbildung4. The model of the proteasome with two cleavage centers. A protein with unspecified sequence (denoted as "0-0-0-0") enters the single proteasome channel from the left. It can be cleaved at any point by cleavage sites denoted by scissors. The cleaved fragments move with different velocities depending on their length. After a waiting time, computed by means of a Gillespie algorithm, either cleavage or translocation may occur.

When the efflux rate and the cleavage rate have a similar time scale we observe three peaks in the distribution of fragments (see 3B). Similar to what is observed experimentally [14], the third peak is much smaller than the other two, and the second peak is larger than the first peak. In our model, the first peak corresponding to the small fragments reflects an efficient cleavage mechanism where fragments are repeatedly cleaved before they are released from the CP. These "rest" products do not collapse to single amino acids because cleavage of very short fragments is improbable in our model (see 1B). The second peak corresponding to fragments with a length of $8-10$ aa, is the result of the preference to cut at $\mu = 9$ aa. Fragments are found in a broad peak around 9 aa, because of the variation in the cleavage (i.e., standard deviation of the Gaussian function). The third peak around 25 aa found in the WT distribution is due to the efflux function. It results from the high probability of a fraction of intermediate 25-35 aa fragments to exit the proteasome. As they would have been a source for fragments of length 15-25 aa, the production of fragments of this length drops. This intuitive explanation elucidates the presence of the third peak.

2 A transport model of the proteasome

The model. The transport model assumes that the proteasome has one channel only and two cleavage centers, i.e. a symmetric structure as seen experimentally. The two cleavage centers represent the projection on the translocation route of cleavage centers of two internal rings, which in reality can have up to 6 cleavage centers but distributed in the 3D structure. The substrate, which enters this channel can be cleaved or translocated as well as generated fragments until they leave the channel (see Fig.4). The translocation and cleavage are modelled by the Gillespie algorithm according to the translocation and cleavage rates [8]. According to this algorithm we can stochastically model the system where several events can happen with different probabilities.

The peptide or its part inside the proteasome can either be shifted by one amino acid or it can be cleaved if it is located near the cleavage center. In this version of the model, outrunning of fragments is forbidden, in the same way as the peptide cannot be translocated into a position already occupied by another fragment. Inside the proteasome, the translocation rates of the substrate or frag-

Parameter	Description	Dimension	Default value
l	Fragment length	Amino acids	-
L_p	Protein length	Amino acids	300
L	Proteasome length	Amino acids	80
D	Distance between a cleavage center and the proteasome end	Amino acids	15
N	Number of degraded proteins	-	10^4

Tabelle2. Parameter values of the transport model

ments depend only on their lengths and are described by the translocation rate function $R_t(l)$, where l is the length of the substrate or fragment part which is inside the proteasome. Hence if the initial substrate enters the proteasome, this length will be increased. According to this function the fragments of different length can have different translocation rates. The probability of cleavage is described by the function $R_c(p)$, where p is the position in the substrate sequence. For generated fragments the cleavage rates remain the same as they were in the initial substrate for the corresponding positions. We assume that the substrate is degraded by a processive mechanism, i.e., the protein cannot move back or cannot leave the proteasome from the other side until completely processed (for experimental argumentation see [1]). When the protein is degraded, its fragments lengths are counted in the length distribution. To obtain reliable statistics, the length distribution is averaged over large number of proteins N. This also corresponds to the usual experimental set up. For parameters see Tabel 2.

Results. First, let us fix all the cleavage rates $R_c(p)$ to a constant and show that different translocation rates can result in qualitatively different forms of length distribution. To check different translocation rate functions, we have used a decreasing function $R_t(l) = R1(l) = 1/l$ and a nonmonotonous function $R_t(l) = R2(l) = (0.5l)^3 e^{-\alpha l}$ with $\alpha = 0.54$ (Fig. 5 left). If the cleavage rates are relatively high $R_c(p) = 0.01$, the difference in the length distribution will be not so much pronounced because the probability of cleavage will dominate over the probability of translocation and, as a result, short fragments will dominate in the length distribution. For both translocation rate functions the length distribution is a monotonously decreasing function.

The situation qualitatively changes if cleavage rates are not so high, e.g. $R_c(p) = 0.001$ (see Fig 6). For a monotonously decreasing function, the length distribution is also monotonously decreasing (left). However for the translocation rate function with the optimal length of transportation, one can clearly see a peak in the length distribution (right). Hence translocation rate dependencies can be of a crucial importance for the length distributions. If this function is nonmonotonuos and has a clearly defined optimal transportation length, this can result in a single peak length distribution as observed in numerous experiments [18,17,12,2]. Since namely the length corresponding to this peak is the most important length for the immune system, we conclude that translocation properties of the protein should be taken into account in the creation of the

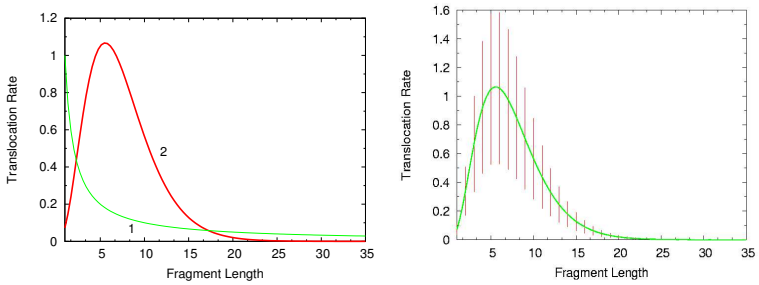

Abbildung5. Left: Two qualitatively different forms of translocation rates used in the model (see Sec. 2), a monotonously decreasing function $R1(l)$ (curve 1) and a non-monotonous function $R2(l)$ with one maximum at the most optimal for translocation length. For exact expressions see the text; Right: Translocation rate function $R2(l)$ and the intervals of its random variation (vertical bars).

virtual proteasome system. Interestingly, tuning the parameters, namely setting $R_t(l) = R2(l)$, $\alpha = 0.47$, and $D = 20$ one can also obtain a three peak length distribution (see Fig. 7, left) found in the experiment [14].

A question naturally arises: what is a mechanism behind such translocation rates? In [28] we have assumed that the proteasome has a fluctuationally driven transport mechanism and shown that such a mechanism generally results in a nonmonotonous translocation rate. Since the proteasome has a symmetric structure, three ingredients are required for fluctuationally-driven translocation: the anisotropy of the proteasome-protein interaction potential, thermal noise in the interaction centers and the energy input.

Proteins and especially unfolded synthetic peptides have indeed a periodic constituent in the potential due to a peptide bond. However this periodicity can be hidden by an unperiodic, sequence specific potential. In this case the real translocation rates for different fragments vary around the function computed for a non-sequence specific case. Let us analyze how much this variation can change the length distribution. For this we perform simulations with all parameters as in Fig. 6 right, but on all simulation steps we change the translocation rates randomly up to 50% of its initial value determined by the function $R2(l)$ (see Fig. 5, right). This means that at any step i the translocation rate for the fragment of the length l_i is equal to $R2(l_i)(1+R_i)$ where R_i are random numbers uniformly distributed in the interval $[-0.5 : 0.5]$. Surprisingly, we have found that in this case the length distribution is exactly the same as in Fig. 6 right (not shown here). Hence, despite the real nonperiodicity of the potential the nonperiodic constituent is not so important for the length distribution as the periodic one, which defines the nonmonotonous rate dependence. Surely, this is true for rather long proteins ($L_p > 150$) and large statistics $N > 10^4$.

The next important question is the influence of the sequence specific cleavage strength. Let us simulate the degradation of the Casein as in [14] with constant cleavage rates and with sequence specific cleavage rates computed with Netchop

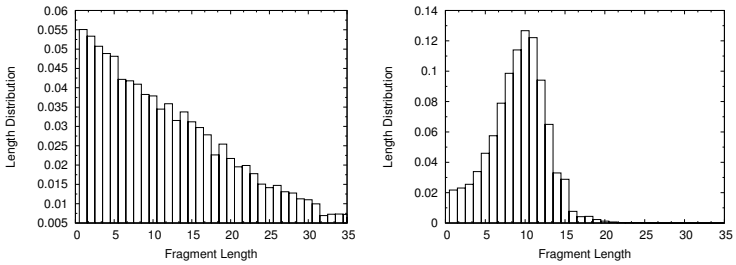

Abbildung6. Length distribution for $R1(l)$, $R_c(p) = 0.001$ (left) and for $R2(l)$, $R_c(p) = 0.001$ (right). It can be clearly seen that nonmonotonous translocation rate can result in one peak distributions.

algorithms. Casein has a length of $L_p = 188$ aa and the cleavage pattern as in in Fig. 7 right. All other parameters are the same as in the case of the three peak length distribution, see Fig. 7 left. We have rescaled the cleavage strength to have the same mean value of 0.001. To our surprise the length distributions of not sequence specific case and sequence specific case are practically identical (not shown). Hence to model the length distribution as a result of different translocation rates, it is not so important to consider the cleavage pattern of the substrate. However, for shorter substrates the cleavage pattern can significantly change the length distribution.

3 Discussion

This work provides insights on the kinetic and translocation properties of the proteasome degradation. A realistic choice for the models parameters is hard to obtain. Both model are phenomenological and designed to qualitatively capture the main features of the kinetics and transport. It is important to note that there is no contradiction between these two models, the kinetic model operates on the mesoscopic scale whereas the transport model on the microscopic one. Hence, the transport model can be included inside the parameters of the kinetic model. At the present stage the modelsdiscussed cannot be used for quantitative predictions and serves as an explanation of the proteasome product size distribution. We identify two possible directions which can be taken in order to develop these models to be able to perform quantitative predictions. A first possibility would be to simulate a population of proteasomes, each of them modeled with the Gillespie algorithm, as in the transport model. A second option would be to take into account the length dependent protein transport correction in kinetic models of the proteasome function, as in [20,16]. In both cases, one should implement a specific protein sequence, which certainly influences a cleavage pattern and the proteasome-protein interaction potential, and description of in- and outfluxes, taking into account the possibility of gate opening and closing [14].

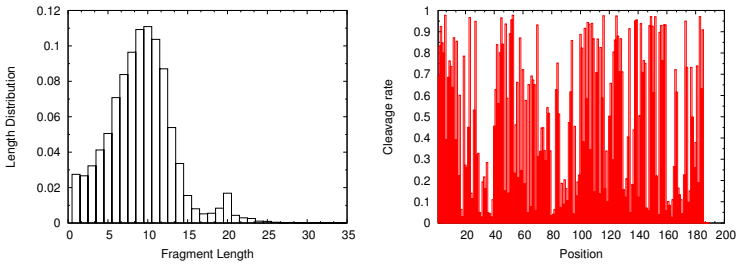

Abbildung7. Length distribution as a result of Casein degradation, with non sequence specific cleavage rates (left). Casein cleavage strength pattern computed with Netchop. (right).

Acknowledgments. FL thank the Australian Research Council through the Discovery Grant scheme (DP0556732 and DP0664970) for funding. AZ acknowledges a financial support from the VW-Stiftung and from the European Union through the Network of Excellence BioSim, Contract No. LSHB-CT-2004-005137.

Literatur

1. T. N. Akopian, A. F. Kisselev, and A. L. Goldberg. Processive degradation of proteins and other catalytic properties of the proteasome from *thermoplasma acidophilum*. *The Journal of Biological Chemistry*, 272:1791–1798, 1997.
2. P. Cascio, C. Hilton, A. F. Kisselev, K. L. Rock, and A. L. Goldberg. 26s proteasomes and immunoproteasomes produce mainly n-extended versions of an antigenic peptide. *EMBO J.*, 20:2357–2366, 2001.
3. A. Ciechanover. The ubiquitin-proteasome proteolytic pathway. *Cell*, 79:13–21, 1994.
4. I. Dolenc, E. Seemuller, and W. Baumeister. Decelerated degradation of short peptides by the 20S proteasome. *FEBS. Lett.*, 434:357–361, 1998.
5. W. Ebeling and R. Feistel. *Evolution of Complex Systems: Self-Organization, Entropy and Development*. Kluwer Academic Pub., 1989.
6. W. Ebeling, L. Schimansky-Geier, and T. Poeschel, editors. *Stochastic Dynamics*. Springer Verlag, 1997.
7. W. Ebeling, L. Schimansky-Geier, and Y.M. Romanovsky. *Stochastic dynamics of reacting biomolecules*. World Scientific Pub Co Inc, 2003.
8. D.T. Gillespie. A general method for numerically simulating the stochastic time evolution of coupled chemical reactions. *J. Comput. Phys.*, 22:403–434, 1976.
9. A. L. Goldberg, P. Cascio, T. Saric, and K. L. Rock. The importance of the proteasome and subsequent proteolytic steps in the generation of antigenic peptides. *Mol. Immunology*, 39:147–164, 2002.
10. M. Groll and R. Huber. Substrate access and processing by the 20S proteasome core particle. *Int. J. Biochem. Cell. Biol.*, 35:606–616, 2003.
11. H. G. Holzhütter and P. M. Kloetzel. A kinetic model of vertebrate 20s proteasome accounting for the generation of major proteolytic fragments from oligomeric peptide substrates. *Biophysical Journal*, 79:1196–1205, 2000.

12. A. F. Kisselev, T. N. Akopian, and A. L. Goldberg. Range of sizes of peptide products generated during degradation of different proteins by archaeal proteasomes. *J. Biol. Chem.*, 273:1982–1989, 1998.
13. P. M. Kloetzel. Generation of major histocompatibility complex class i antigens: functional interplay between proteasomes and tppii. *Nature Immunology*, 5:661–669, 2004.
14. A. Köhler, P. Cascio, D. S. Leggett, K. M. Woo, A. L. Goldberg, and D. Finley. The axial channel of the proteasome core particle is gated by the rpt2 atpase and controls both substrate entry and product release. *Molecular Cell*, (7):1143–1152, 2001.
15. B. Lankat-Buttgereit and R. Tampe. The transporter associated with antigen processing: function and implications in human diseases. *Physiol Rev*, 82:187–204, 2002.
16. F. Luciani, C. Kesmir, M. Mishto, M. Or-Guil, and R. J. de Boer. A mathematical model of protein degradation by the proteasome. *Biophysical Journal*, 88:2422–2432, 2005.
17. A. Nussbaum. *From the test tube to the World Wide Web: The cleavage specificity of the proteasome*. PhD thesis, Eberhard-Karls-Universitaet Tuebingen, 2001.
18. A. K. Nussbaum, T. P. Dick, W. Kielholz, M. Schirle, S. Stevanovic, K. Dietz, W. Heinemeyer, M. Groll, D. H. Wolf, R. Huber, H. G. Rammensee, and H. Schild. Cleavage motifs of the yeast 20s proteasome β subunits deduced form digests of enolase 1. *Proc. Natl. Acad. Sci. USA*, 95:12504–12509, 1998.
19. R. Z. Orlowski. The role of the ubiquitin-proteasome pathway in apoptosis. *Cell Death Differ.*, 6:303–313, 1999.
20. B. Peters, K. Janek, U. Kuckelkorn, and H. G. Holzhütter. Assessment of proteasomal cleavage probabilities from kinetic analysis of time-dependent product formation. *J. Mol. Biol.*, 318:847–862, 2002.
21. B. Peters, K. Janek, U. Kuckelkorn, and H. G. Holzhutter. Assessment of proteasomal cleavage probabilities from kinetic analysis of time-dependent product formation. *J. Mol. Biol.*, 318:847–862, 2002.
22. G. Schmidtke, S. Emch, M. Groettrup, and H. G. Holzhuetter. Evidence for the existence of a non-catalytic modifier site of peptide hydrolysis by the 20s proteasome. *J. Biol. Chem.*, 275:22056–22063, 2000.
23. N. Shastri and S. Schwab. Producing nature's gene-chips: the generation of peptides for display by mhc class i molecules. *Annu. Rev. Immunol.*, 20:463–493, 2002.
24. R. L. Stein, F. Melandri, and L. Dick. Kinetic characterization of the chymotrypic activity of the 20s proteasome. *Biochemistry*, 35:3899–3908, 1996.
25. R. Stohwasser, U. Salzmann, J. Giesebrecht, P. M. Kloetzel, and H. G. Holzhuetter. Kinetic evidence for facilitation of peptide channelling by the proteasome activator pa28. *Eur. J. Biochem.*, 267:6221–6230, 2000.
26. T. Wenzel, C. Eckerskorn, F. Lottspeich, and W. Baumeister. Existence of a molecular ruler in proteasomes suggested by analysis of degradation products. *FEBS Letters*, 349:205–209, 1994.
27. A. Zaikin and J. Kurths. Optimal length transportation hypothesis to model proteasome product size distribution. *Journal of Biological Physics*, 2006. accepted for publication.
28. A. Zaikin and T. Pöschel. Peptide-size-dependent active transport in the proteasome. *Europhysics Letters*, 69:725–731, 2005.